Asian Journal of Chemistry; Vol. 31, No. 9 (2019), 2073-2082

ASIAN JOURNAL OF CHEMISTRY

https://doi.org/10.14233/ajchem.2019.22108

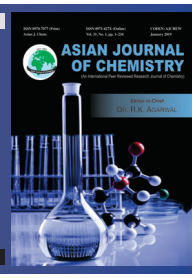

Organic Boronate Affinity Sorbent for Capture of *cis*-Diol Containing Compounds

EMAN ALZAHRANI

Department of Chemistry, Faculty of Science, Taif University, Taif, Kingdom of Saudi Arabia

Corresponding author: E-mail: em-s-z@hotmail.com

Received: 30 March 2019; *Accepted*: 6 May 2019; *Published online*: 31 July 2019; AJC-19500

Boronate affinity chromatography (BAC) is argued to be a critical tool in specific capture and separation of *cis*-diol containing compounds. In present study, organic boronate affinity monolith poly(3-acrylamido phenylboronic acid-*co*-ethylene dimethacrylate) (AAPBA-*co*-EDMA) is prepared through one-step *in situ* polymerization procedure within a micropipette through the application of a pre-polymerization mixture which contains functional monomer (3-acrylamido phenylboronic acid), cross-linker (ethylene dimethacrylate), porogenic solvent (methanol with poly ethylene glycol) and initiator (2,2-dimethoxy-2-phenyl-acetophenone). Following the optimization of time exposure to UV lamp with 365 nm, the macroporous organic boronate monolith was selected. Several approaches including SEM and BET analysis, FT-IR spectroscopy and measuring contact angle were applied in the characterization of the morphology of the monolith. Several *cis*-diol compounds that include catechol and galactose are applied in the assessment of the boronate affinity of the organic monolithic material. Additionally, the capture of glucose from urine sample is also conducted. The basic principle of the approach is that boronic acid forms covalent bond with *cis*-diols in basic solutions whereas the ester bonds are dissociated under acidic media. By using the study results, monolith demonstrate good selectivity towards *cis*-diol containing compounds. Due to the hydrophilic property of monolith, the affinity chromatography monolith can be performed for several *cis*-diol compounds including glycoproteins and nucleosides. Also, fabrication of the organic boronate monolithic in microfluidic equipment is essential in facilitating the extraction of boronate affinity using small-volume samples.

Keywords: Boronate affinity sorbent, Organic monolith, *cis*-Diol, Capture, Urine sample.

INTRODUCTION

Several biomolecules contain a minimum of a single *cis*-diol structure. Some of these biomolecules include saccharides, catecholamines, ribonucleotides and glycolipids. Such *cis*-diol containing biomolecules play an essential role in the living organisms [1-4]. These roles may be either functional or structural which has made them essential in different fields such as metabolomics, proteomics and glycomics. Glycoproteomics is defined as the study of the sites of glycosylation, the analysis of the glycan structure and site occupancy. It also involves the study of the distribution of glycan isoform as well as the quantitative analysis of the glycoproteome. Due to the components of the glycoproteomics, it has become a vital topic for research and also an essential strategy in the discovery of biomarker [2,5-10].

There have however been several challenges linked with glycoproteomics with one such challenge is the low abundance of glycopeptides. Another such reason is the low-efficiency rate of ionization when compared with the non glycopeptides. These factors lead to significant suppression of the mass spectrometric response of the glycopeptides due to the large number of non-glycopeptides [11]. For that reason, it is essential to employ the efficient enrichment approaches before analyzing to help in the isolation and the enrichment of the glycoproteins or glycopeptides [12-14].

Preparing a sample is critical in implementing the overall analytical process as it aids in the extraction and the concentration of the targeted analytes. An additional benefit linked with sample preparation is that it helps in overpowering the matrix interferences whereas enhancing the ability to detect the analytical technique. Some of the preparatory procedures include implementing pretreating the sample through extraction which is solvent and sorbent based. It is essential to note that the sorbent-based extraction is increasingly famous compared to the solvent-based strategy as it applies minimum toxic solvent [15-17].

There has been an increased interest in boronate affinity (BA) chromatography for the past few years as it is perceived to be an effective approach in implementing selective preparation or the enrichment of *cis*-diol containing biomolecules [18-21]. Such effectiveness in the performance of boronate affinity materials has been boosted by the application of the special boronic acid ligands including the Wulff-type boronic acids [22,23], the boronic acids containing electron-withdrawing groups [24,25] and also the benzoboroxoles [26-28].

It is essential to note that asides from the pivotal role played by the boronate ligands, the type of the supporting materials significantly impact the ability of the boronate affinity materials to bind [29]. There are several formats that can be adopted by supporting materials which is mainly reliant on different applications. Some of these formats including mesoporous materials [30], nanoparticles [31,32], monoliths [33-37] and molecularly implemented polymers [38,39]. There has been rapid development of the boronate affinity monolithic columns which can be significantly attributed to the merit of both the boronate affinity and monolithic columns. The porous polymeric monoliths has been identified as occupying vital position in separation science owing to the reduced costs, simple fabrication, high rate of mass transfer and also the high tolerance to the extreme pH levels [40]. There has also been rapid development in the boronate affinity monoliths which can be attributed to the combination of unique selectivity of the boronate affinity materials. For that reason, boronate affinity has been identified as being unique manner for selective recognition and enrichment of the *cis*-diol containing molecules. The method is based on the principle that there is reversible covalent complex formation or dissociation among the boronic acids and the *cis*-diol containing compounds among the alkaline or acidic aqueous solutions. The ability of pH to switch has led to boronic acids being excellent ligands in several concepts [41-43].

In current research, the poly(3-acrylamido phenylboronic acid-co-ethylene dimethacrylate) poly (AAPBA-co-EDMA) monolithic column has been synthesized by the *in situ* free radical polymerization in a micropipette. The impact of the radiation time among the established monoliths was examined. The size and the morphology of the sorbent has been characterized through the use of several techniques including SEM analysis, infrared spectroscopy, BET analysis, EDX analysis and also measuring the contact angle. The fabricated monolithic column has been applied in capturing the *cis*-diol containing molecules that may include carbohydrates and catechol through the use of one-step *in situ* polymerization procedure. Additionally, fabricated organic monolithic materials have been used in capturing glucose from the urine sample.

EXPERIMENTAL

The materials to be used for the experiment were acquired from Fisher Scientific located in Loughborough in the United Kingdom. Some of these materials include sodium hydroxide solution, hydrochloric acid, 3-acrylamidophenylboronic acid (AAPBA) and ethylene dimethacrylate (EDMA). Other items used in the experiment were acquired from Tokyo Chemical Industry. Such materials include acetone methanol and polyethylene glycol (PEG). Additional materials include 3-(trimethoxysilyl)propyl methacrylate (γ-MAPS), 2,2-dimethoxy-2-phenyl-acetophenone (DMPA), galactose, catechol and glucose were acquired from Shangai Chemical in China. Materials acquired from Kinesis in Cambridge in the United Kingdom include the plastic syringes where phosphate buffer, glacial acetic acid and acetonitrile were acquired from Scientific Laboratory supplies.

Electrical tape was bought from Onecall in Leeds whereas a micropipette was acquired from the lab ware house in London in the UK. Sonicator from Ultra wave Sonicator U 300HD UV lamp producing 365 nm was acquired from Spectronic Analytical Instruments bought from Leeds whereas scanning electron microscope (SEM) Cambridge S360 from Cambridge Instrument located in Cambridge in the UK. Other materials acquired include a pH meter from Fisherman hydrus 300 and a Thermo Orion in Beverly, in the US. Additionally, a syringe pump was bought from Bioanalytical System Inc. situated in West Lafayette, USA. A Nitrogen adsorption-desorption measurements were set at 77 K on an ASAP2020 instrument which was purchased from Micromerities which is situated in Norcross, in Georgia in the US. The FT-IR spectra used in the present study were Perkin Elmer RX FTIR × 2 with diamond ATR and also DRIFT attachment from Perkin Elmer acquired from Buckinghamshire in the UK. The HPLC analysis was conducted while using a Perkin Elmer LC200 series binary pump.

Preparation of the AAAPBA-*co*-EDMA monolith: The fabrication of a monolith which is based on a polymer was performed inside a micropipette (200 μm i.d.). Additionally, the connection of the micropipette to a 1 mL plastic syringe was implemented through the use of a microtight through a syringe driver for adjusting the flow rates. A syringe pump with a flow rate of 2 μL min^{-1} was used to inject the different solutions. Treating of the micropipette with vinyl salinizing agent according to a method in a method which has been outline was implemented to help in covalently anchoring the polymer to micropipette wall [44]. Initially, the rinsing of the micropipette to be used using a 1 M of NaOH solution for 1 h through the use of a syringe pump was conducted followed by the use of distilled till the pH value of the outlet solution was 7.0. Afterwards the drying of the micropipette in an oven set at 45 °C was performed for 24 h.

γ-MAPS was used in salinizing the inner walls of the micropipette. Such surface silanization is attained through washing of the micropipette using a solution that comprise of 20 % (v/v) γ-MAPS which is dissolved in 95 % ethanol set at a pH value of 5 having a glacial acetic acid [45]. Later, the solution was inserted into a tube through the use of a syringe pump for 1 h. Following the surface vinylization, the micropipette was then rinsed using acetone after which it was dried through the use of stream of nitrogen gas. The micropipette was then left for 24 h after which was set for polymerization reaction.

The components of the polymerization mixture are outlined in Table-1. Photoinitiated free radical polymerization is used in preparing the polymer-based monolith inside a micropipette at a room temperature in a UV radiation. The polymerization mixture is made up of 60 mg of AAPBA, 140 mg of EDMA solution and 20 mg of photoinitiator. The porogenic

TABLE-1
COMPOSITIONS OF THE POLYMERIZATION MIXTURE APPLIED IN PREPARING THE ORGANIC BORONATE AFFINITY MONOLITH

Type	Chemical	Weight (mg)
Monomer	3-Acrylamidophenylboronic acid (AAPBA)	60
Crosslinker	Ethylene dimethacrylate (EDMA)	140
Porogenic solvent	Polyethylene glycol :methanol (PEG :MeOH)	70:530
Photoinitiator	2,2-Dimethoxy-2-phenyle-acetophenone (DMPA)	20

solvent on the other hand, comprises of PEG and MeOH measuring 70 and 530 mg, respectively. Sonication of the mixture was performed for a period lasting for 5 min with aim of deriving homogeneous solution.

Later, the mixture was inserted into a micropipette through the usage of a syringe pump. Blu tack was used to seal the ends of the micropipette and later exposed to a UV lamp (365 nm) with the distance between the two being 2 cm. Although the rest of the micropipette was covered using an electrical tape with aim of safeguarding against the formation of the monolith through the complete micropipette, only a centimeter of the micropipette was subjected to UV radiations. The test were conducted at different times including 20, 30 and 40 min. Following the completion of polymerization reaction, a syringe pump of MeOH was used in flushing the monolith tube for a period of 12 h. The action was performed to get rid of the unreacted components and the porogenic solvents from the monolith.

Characterization of the boronate affinity monolith

SEM analysis: Characterization of the morphology of the dried monolith was conducted through scanning electron microscopy (SEM) that applies a Cambridge S360 scanning electron microscope acquired from Cambridge Instruments, UK. The images were acquired by the application of an accelerating voltage of 20 kV and a probe current of 100 pA under high vacuum mode. The gold platinum with a thickness of around 2 nm were used to coat the samples using a thin layer. The process will use SEMPREP 2 Sputter Coater acquired from Nanotechnology Ltd. located in Sandy in the UK.

BET analysis: Measurement of the N_2 isotherms at 77 K was performed to implement the BET analysis using the surface area and average diameter as the BET parameter. The different samples were outgassed at 400 K in vacuum for a period of 6 h.

FT-IR spectroscopy and contact angle measurement: The collection of the FT-IR spectra was performed in the attenuated total reflectance (ATR) mode. Six scans having a resolution of 4 cm^{-1} were conducted with the IR range of 4000 to 500 cm^{-1}. Preparation of monolith was performed in a centrifuge tube of 1.5 mL under identical conditions with the aim of assessing the FT-IR absorbance of the boronate affinity monolith. The extraction of Soxhlet was performed with water and methanol after a period of 24 h following the cutting of the bulk materials to small pieces after which it was dried in a vacuum of 90 °C. These pieces were then grounded into fine powders after which an appropriate quantity of potassium bromide was added. A small quantity was then squeezed into a thin disk and after that the measurement of FT-IR collected. An additional disk was also pressed without potassium bromide and then later implemented the contact angle measurement.

Capture of *cis*-diol compounds: Capturing of the *cis*-diol compounds such as galactose and catechol was done independently to facilitate the calculation of the recovery following the extraction of every compound. An investigation of the boronate affinity monolithic column was done through the use of 400 µL of MeOH. It was later equilibrated using 400 µL of a loading buffer which was made up of 50 % acetonitrile and 10 mM phosphate buffer solution with a pH value of 8.5. Later, the dissolution of the 800 µL of sample solution dissolved into phosphate buffer solution (pH 8.5) was then inserted into the monolithic column. The next step involved washing the micropipette with 150 µL of 50 % acetonitrile and 10 mM phosphate buffer solution with a pH value of 8.5. The final step involves conducting the elution of preconcentrated analyte and regeneration of the column through the application of 200 µL of 50 % (v/v) acetonitrile as well as 100 mM acetic acid buffer solution with pH value of 2.7. The combination of these processes was done to facilitate the extraction of *cis*-diol containing compounds through the organic affinity monolith. The process is outlined in Table-2. During the procedure, the insertion of the solutions into micropipette was done using the syringe pump at a flow rate of 10 µL min^{-1}.

Collection of the effluent was done in the Eppendorf tube and later analyzed through the use HPLC-UV detection. Isocratic elution was performed with (v/v) 50 % acetonitrile and distilled water, the flow rate was 0.3 mL min^{-1} and the injection volume was 20 µL. The separation column was symmetry C8, 4.6 mm × 250 mm packed with silica (size 5 mm). Between consecutive analyses, a needle for the automated injector was washed with 70 % aqueous methanol. The goal of the HPLC-UV detection was to support the the peak area collected for the preconcentrated compound and also facilitate

TABLE-2
PURIFICATION PROFILE OF *cis*-DIOL CONTAINING COMPOUNDS USING THE BORONATE AFFINITY MONOLITH

Step	Volume (µL)	Solution
Activation	400	Methanol
Equilibration	400	50 % (v/v) acetonitrile and 10 mM phosphate buffer solution (pH 8.5)
Apply sample	800	*cis*-Diol compound was dissolved in 10 mM phosphate buffer solution (pH 8.5)
Washing	150	50 % (v/v) acetonitrile and 10 mM phosphate buffer solution (pH 8.5)
Elution	200	50 % (v/v) acetonitrile and 100 mM HAc (pH 2.7)

for the comparison with the other peak areas for the analyte standard solutions which have not been processed thus allowing for the calculation of the extraction recovery (ER) through the use of the equation provided by Alzahrani [15,17,46,47] below:

$$\text{Extraction recovery (\%)} = \frac{I_{elute}}{I_{total}} \times 100$$

where, I_{elute} signify the content eluted form the sorbent, whereas I_{total} is the composition of analyte which is inserted into the sorbent.

Purification of glucose from real sample: Healthy volunteers provided samples of healthy urine. One provision was that the volunteers needed to be aged between 18 and about 60 years old. Additionally, they should be healthy with no major illnesses, healthy weight and do not smoke. The content urine sample from a healthy worker obtained measured 45 mL. The non-first morning urine sample was then frozen and stored at -20 °C. Before initiating the analysis, thawing of the urine sample was performed at room temperature. A small content of the urine sample measuring 10 mL aliquot was centrifuged for a period of 30 min with a rate of 6000 rpm lasting 8 min. In addition, the supernatant was obtained to facilitate for further analysis. Additionally, checking the organic boronate affinity sorbent performed through the use of a spiked sample using glucose through the similar pattern outlined as above.

RESULTS AND DISCUSSION

Optimization of boronate affinity monolith fabrication: The usage of boronate affinity chromatography is identified to be powerful in implementing selective separation and enrichment of the *cis*-diol containing compounds from sample matrix. The molecular reaction between the different boronate affinity materials is dependent on the reversible covalent reaction between boronic acid ligands and *cis*-diol containing compounds [48-51].

In this work, the fabrication of hydrophilic boronate functionalized polymeric monolithic material in the a micropipette was performed through the *in situ* polymerization. The decision in selecting monolithic materias to function as sorbent bed is based on their easier fabrication, low back pressure and quick convective mass transfer [52].

The initial stage towards creating organic polymer-based monolithic stationary phases in the micropipette is based on the pretreatment of the micropipette. The procedure was performed to allows for cleaning and activating the inner surface walls of the micropipette done by washing it with acetone, which removes organic materials. It was later rinsed using water to allow for flushing out the remaining acetone. The application of basic solution such as KOH or NaOH can be effective in hydrolyzing the siloxane bridge and forming silanol groups [45]. For the present study 0.2 M NaOH is applied in activating the surface of the micropipette.

The process was followed by cleaning the micropipette through the application of deionized water as it is effective in the removal of remains of basic solutions. The final step include cleaning the 0.2 M HCl in neutralizing and eliminating the alkali metal ions [53].

Following the activation of the micropipette surface, the salinization was performed prior to the fabrication of the boronate monolith material inside the micropipette. The silanization is beneficial in that it allows for covalent attachment of the monolith, thus eliminating the effect of shrinkage during the polymerization reaction. The process also facilitates preventing undesired for the analytes using the silanol groups of the micropipette [54]. Salinizing the surface micropipette is meant to promote static coating through the usage of silanizing agent (γ-MAPS) as it is a bifunctional agent and is capable of binding to trimethoxysilane functional groups using covalent bond to the silanol (Si-OH) groups in the micropipette for the salinizing agent. The participation of the methacrylate in the polymerization reaction contributed to the biding of the continuous beds through the covalent bonding in the inner wall of the micropipette [55].

The mechanism of the formation of the AABPA-*co*-EDMA polymer is shown in Fig. 1. The synthesis of the boronate functionalized monolith through polymeric reaction comprises of (DMPA) as a starter for free-radical polymerization. Copolymerization of the hydrophilic monomer (AABPA) alongside (EDMA) is performed as a hydrophobic cross-linker subjected to UV lamp (365 nm). The high hydrophilic nature of AABPA presents excellent specificity whereas enabling the avoidance of the high concentration of organic solvent during the mobile phase. As a result of the huge surface area, AABPA has demonstrated a huge capability to bind [56]. The ability to obtain a porogen solvent has been identified to be vital in enabling the formation of polymeric monolith. Although the monomer is a polar compound, it possesses poor solubility capability during weak polar solvents. Taking into concept the presence of hydroxyl groups under the monomer (AABPA), ethylene glycol was selected as a form of combination of the mixture of porogenic solution. It was effective porogen in the formation of porous poly (AABPA-*co*-EDMA) monolith [29].

Even though the process of preparing the monolithic stationary phases is simple, there are several factors that need to be taken into consideration. Selecting the porogenic solvent is also an essential element in preparing the monolithic stationary phases. Firstly, the initiator, monomer and cross-linker have to be soluble in the porogenic solvents. Secondly, the porogenic solvents should produce large pores, in order to assure good flow-through properties of the resulting polymer. In this study, PEG (70 mg) and MeOH (530 mg) were used as porogenic solvent. The reaction of the free radical polymerization is started by the usage of the UV light under the photoinitiation process, which is implemented at room temperature instead of using a water bath which is normally implemented under the thermal initiation process [57-60]. The decision to select photoinitiation approach in preparing the organic monolith is based on an understanding that the appropriate length of micropipette is subjected to the light source and as a result, can be easily controlled through the application of masking tape for the remaining tube section which would in turn help in fabricating the polymer-based monolith within the micropipette. The timeline for the exposure to UV light significantly influences the structure of the monolith and the various characteristics for separation.

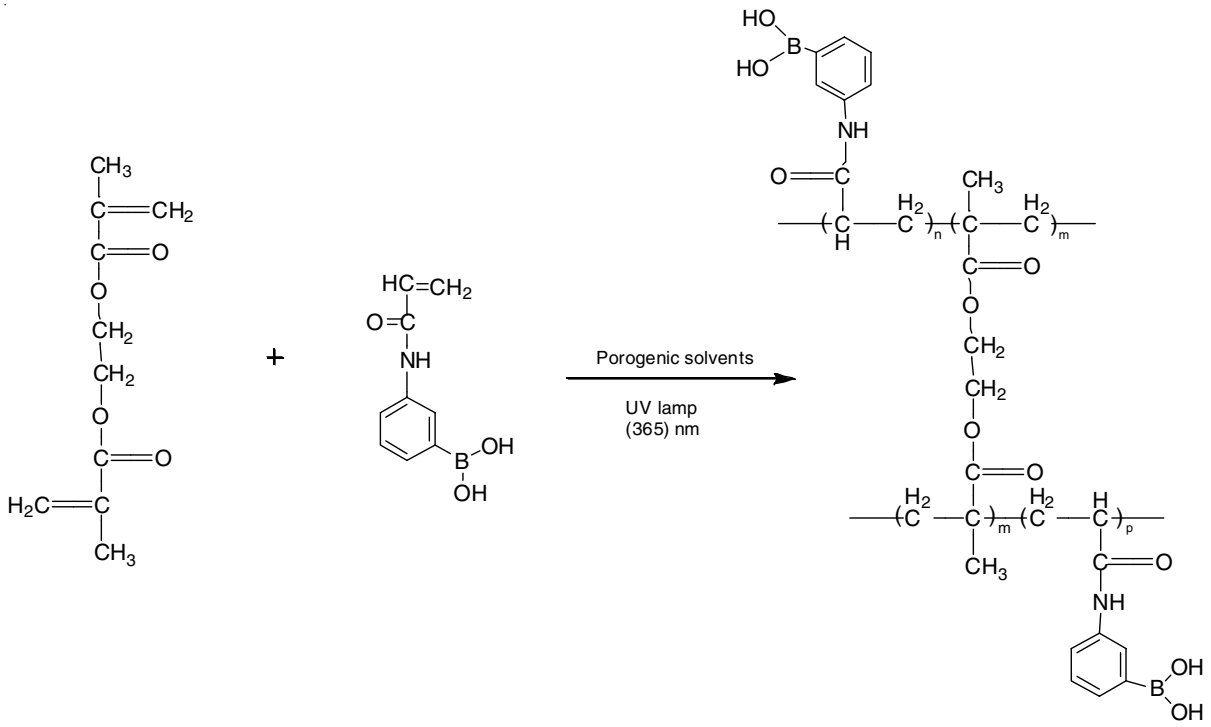

Fig. 1. Reaction mechanism of free radical polymerization of (AAPBA-*co*-EDMA) monolith

The impact of the exposure period to the UV light for the boronate affinity polymer-based monolith is assessed in the present paper with a timeline of 20, 30 and 40 min. The goal is to select the most appropriate timeline to fill the polymerization reaction as outlined in Fig. 2. The formation of continuous beds can be effectively reflected through the appearance of porous polymer monolith, which appears like a bright white material [61]. The initial conclusion to be made can be associated with the impact of the polymerization timeline during the formation of the organic monolith. Observation was made that an exposure lasting 20 min was insufficient in fabricating organic monolith in the micropipette. An increase in exposure time to 40 min identified no difference in the white solid monolithic material in the micropipette. However, the monolithic polymer tube could not be washed through the use of syringe pump which can be attributed to the generation of smaller pores and low permeability of the monolith linked with increasing duration of exposure to the UV light [62]. A conclusion can be made optimum time for to place polymer-based monolith in the tube is 30 min since the polymeric monolithic stationary phases was effective in comparison with the other monoliths. Additionally, the monolithic micropipette could still be cleaned after a 30 min exposure.

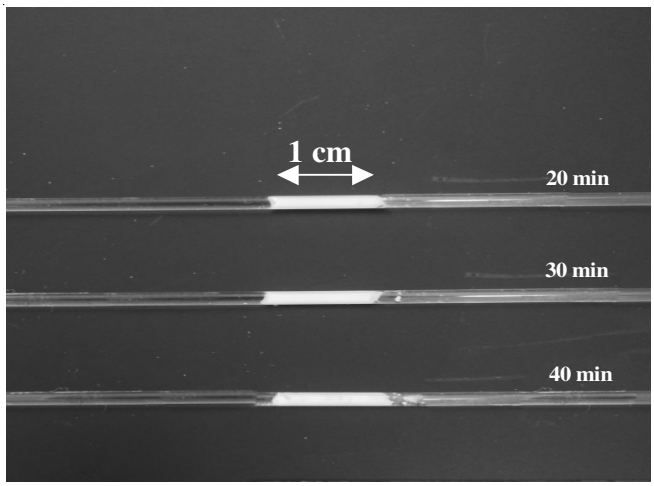

Fig. 2. (AAPBA-*co*-EDMA) monolith was synthesized inside a micropipette by *in situ* polymerization using different irradiation time

Characterization of the organic boronate monolith

SEM analysis: SEM analysis characterized morphology of the resulting monolith when exposed to the optimum preparation conditions. The hybrid monolith that comprise of an ongoing network and uniform pore distribution was obtained. The cross-section morphology for the monolith was homogeneous as reflected in Fig. 3.

BET analysis: The BET approach was adopted in measuring the exact surface area and the average pore size using the adsorption data in the relative pressure with a range between 0.01 to 0.99. The surface area for the AAPBA-*co*-EDMA monolith was calculated as 45.8 $m^2 g^{-1}$ whereas the average pore size of the AAPBA-*co*-EDMA monolith was calculated to be 7.11 nm. Additionally, the column permeability for the fabricated materials was calculated to be 2.5×10^{-13} m^2 for water and 2.1×10^{-13} m^2 for ethanol. This study findings point to the swelling and shrinking of the monolithic material in aqueous solution and organic solvent.

FT-IR spectroscopy and contact angle measurement: Fig. 4 outlines the Fourier transform infrared (FT-IR) spectrum for the organic boronate affinity monolithic material. The peaks for stretching of (OH) group is at 3362 cm^{-1} whereas that of bending vibration 1636 cm^{-1}. The amide group can be attributed to the absorption peaks set at 1551 cm^{-1} in spectra. The boronic acid groups [-$B(OH)_2$] can be outlined by the peak at 1353 cm^{-1}. Other peaks include 1717 and 1428 cm^{-1} were contributed

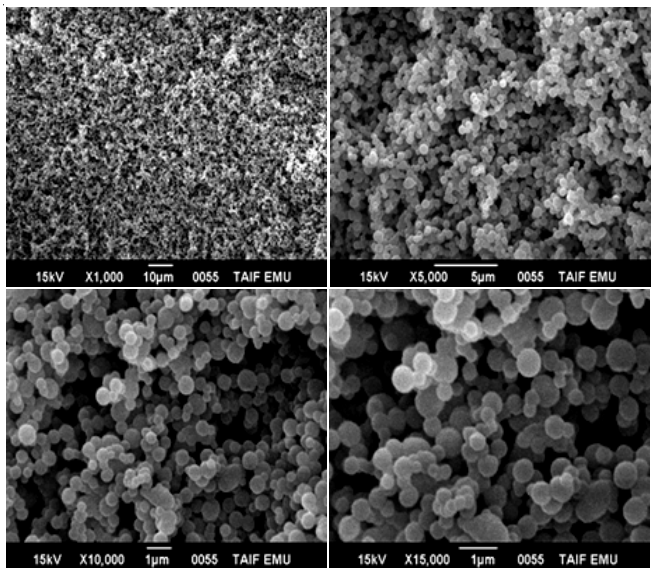

Fig. 3. SEM images of AAPBA-*co*-EDMA boronate affinity monolith

through the stretching vibrations of benzene ring. The stretching band was set at 706 cm^{-1} which is characteristic of *meta*-substitution on benzene ring. The different study results have pointed to boronic acid groups as being successful being incorporated into the monolith.

An investigation of the hydrophilicity of the boronate affinity monolith was implemented by assessing the wetting contact angle. A slim disk of the pressed monolith powders reflects the wetting contact angle estimated to be close to 0° by having a high rate of spreading over the disk surface when a water droplet is released thus signifying the high hydrophilic nature of the monolith.

Applications of the boronate affinity monolith

Capture of carbohydrate and catechol: The aim of the present study is to fabricate the organic boronate affinity monolith for capture of *cis*-diol containing compounds. The results outlined by Table-3 reflect that *cis*-diol compounds were used in assessing the performance of the fabricated boronate affinity monolith. 400 µL of MeOH was used in cleaning the AAPBA-*co*-EDMA monolithic micropipette as it helps in removing the impurities. Equilibration using a loading buffer made of 50 % (v/v) acetonitrile and 10 mM phosphate buffer solution (pH 8.5) was performed with aim of guaranteeing there is sufficient binding of interested analyte. The loading buffer contained a sample solution that contained galactose (16 mg mL^{-1}) which was pumped using a micropipette.

TABLE-3
cis-DIOL COMPOUNDS UTILIZED IN THIS STUDY TO CHECK THE PERFORMANCE OF FABRICATED BORONATE AFFINITY MONOLITH

Name	m.w. (g mol^{-1})	c.f.	Structure
Galactose	180.156	$C_6H_{12}O_6$	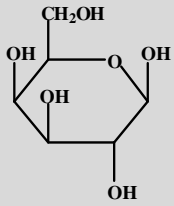
Catechol	110.100	$C_6H_6O_2$	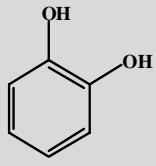
Glucose	180.156	$C_6H_{12}O_6$	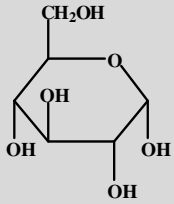

The extraction efficiency is significantly impacted by the sample pH value since the current form of sorbent and analytes are impacted by the sample pH value [63]. Since the boronate affinity chromatography provides for the binding pH buffer to be greater than or equal to the pKa of the boronic acid ligand, which has a moderately low pKa value of AAPBA (8.2). The basic solution selected 10 mM phosphate buffer solution with

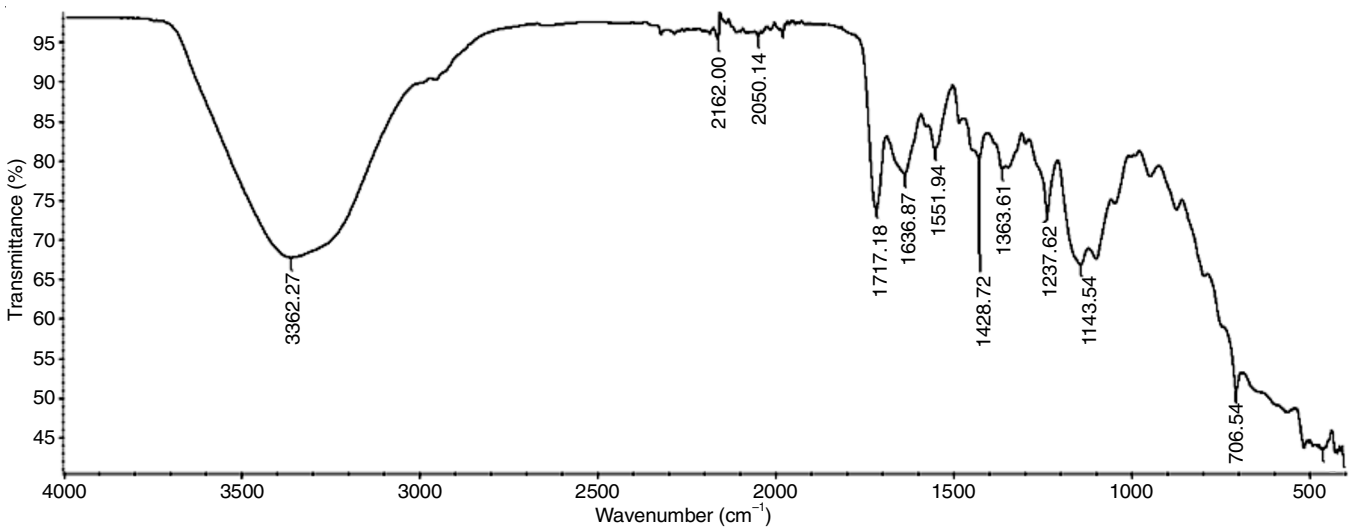

Fig. 4. FT-IR spectrum of AAPBA-*co*-EDMA monolith

a pH of 8.5 as the acid form covalent ester bonds with *cis*-diols in these basic solutions [6,22]. Following the loading of the sample solution using the extraction monolith, rinsing of the sorbent was conducted to facilitate the removal of the interferences whereas ensuring that analyte was not lost.

The addition of an appropriate acid in desorption solvent was essential in disrupting the B-N coordination between sorbent and *cis*-diol compounds and as a result, favouring the desorption of analytes from sorbent [53]. In the current research, the binary solvent are composed of 50 % (v/v) acetonitrile and 100 mM acetic acid buffer solution (HAc) with a pH of 2.7, which was then selected as desorption solvent. Noting that the elution of the *cis*-diol compound is conducted at acidic condition, the strategy fits with the mass spectrometry (MS) by enabling its application in the -omics analyses [64].

Checking of the boronate affinity monolith through the usage of HPLC-UV detector that allows for the comparison of the peak area for every sample, was performed following the preconcentration of the standards of the *cis*-diol compounds. Fig. 5 shows the UV chromatogram for a non-processed galactose sample and the eluent solution of galactose with a retention time of approximately 1.0 min. The figure reflects that the peak height of galactose improved following the capture through the usage of the sorbent which points to the preconcentration of galactose.

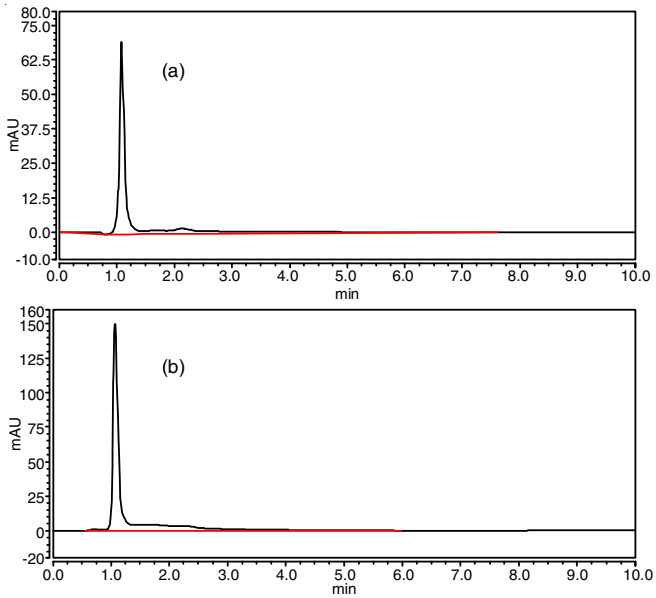

Fig. 5. HPLC chromatograms of standard galactose (16 mg mL^{-1}), direct injection of the standard galactose (a) and after preconcentration using the fabricated organic boronate affinity sorbent (b)

Examination of the performance of the organic boronate affinity within the micropipette was also performed through the use of catechol (8 mg mL^{-1}) using a similar procedure. The UV chromatogram of catechol prior and after the preconcentration that uses fabricated sorbent is demonstrated in Fig. 6. The figure shows that the single intensity of catechol with a peak of approximately 1.7 min improved rapidly following the preconcentration. These results can be used in demonstrating that fabricated boronate affinity monolith sorbent possesses a high extraction capability and selectivity in the *cis*-diol compounds.

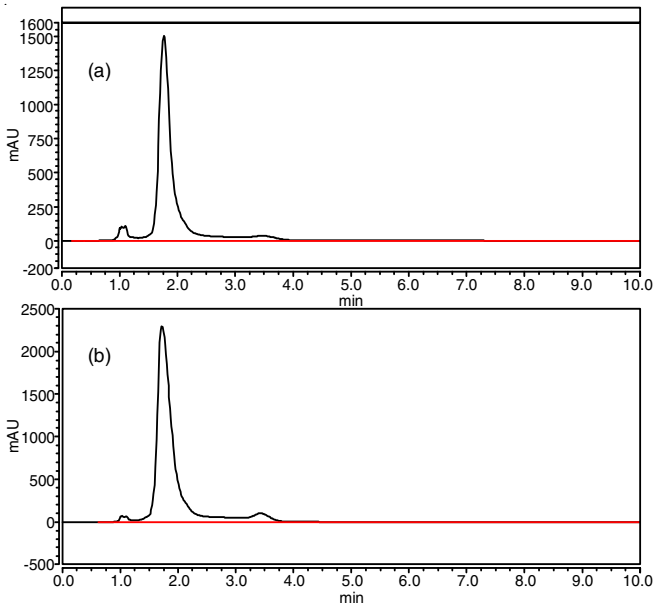

Fig. 6. HPLC chromatograms of standard catechol (8 mg mL^{-1}), direct injection of the standard galactose (a) and after preconcentration using the fabricated organic boronate affinity sorbent (b)

Table-4 further makes a comparison between the peak height and peak area of the preconcentrated galactose and catechol where the usage of the non-process sample solution leads to a significant increase in the peak area and peak height of *cis*-diol containing compounds were following the preconcentration. These results can be applied in drawing a confirmation that there was recovery of the *cis*-diol containing compounds and that the fabricated sorbent possess the potential of eliminating the *cis*-diol containing compounds.

TABLE-4
COMPARISON OF THE PEAK HEIGHT AND PEAK AREA OF THE NON-PROCESSED *cis*-DIOL COMPOUNDS AND AFTER PRECONCENTRATION USING THE BORONATE AFFINITY SORBENT

cis-Diol compound	Retention time (min)	Peak height (mAU)	Peak area (mAU s)
Non-processed galactose	1.05	72.94	8.40
After preconcentration	1.08	149.70	13.29
Non-processed catechol	1.76	1507.16	364.84
After preconcentration	1.71	2296.59	500.16

There is a reversible covalent reaction between boronic acid ligands and *cis*-diol-containing compounds for an alkaline or acidic aqueous solution, which depends on during the principle of molecular interactions of boronate affinity materials. The general formula in the interaction is demonstrated by Fig. 7. Under the formula, with a pH value which is higher than the pKa value of the boronic acid, the boronic acid occurs as a form of a tetragonal boronate anion (sp^3). It is capable of reacting with the *cis*-diols and as a result leading to the formation of five or six-membered cyclic esters. When the solution is acidic, the boronic acid-*cis*-diol complex detaches since the pH condition of the boronic acid is reflected as a trigonal configuration (sp^2). There is limitation in the binding between the sp^2 form of the boronic acid and *cis*-diol-containing compounds [53].

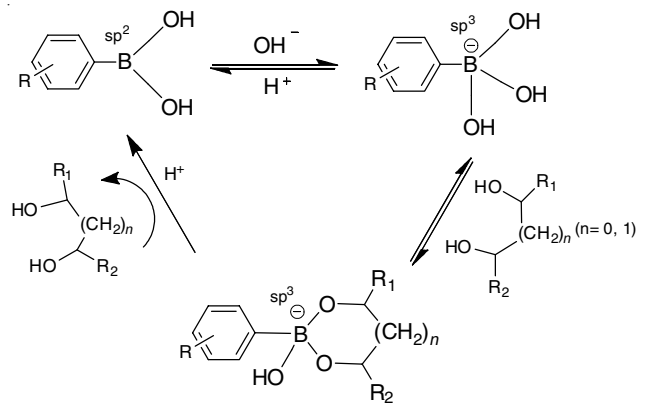

Fig. 7. Schematic of interaction between boronic acids and *cis*-diol containing compounds

Since several of the boronic acid ligands among the affinity materials are aromatic boronic acids, they can potentially contribute to the nonspecific adsorption of high-abundance analyte as a result of the hydrophobic interaction and aromatic π-π interaction. One of the major secondary interactions that impact the selectivity of the boronate affinity is hydrophobic interaction. Most of the boronic acid ligands which are applied among affinity materials are usually aromatic boronic acids and thereby can give rise to hydrophobic interaction and aromatic π-π interaction [64]. That can in turn contribute to the nonspecific adsorption of analytes such as proteins. A solution to the issue is through addition of acetonitrile to the binding buffer with the aim of eliminating the secondary hydrophobic interaction. Since boronic acid tends to transmit hydroxyl groups, the hydrogen binding is an unavoidable secondary interaction.

Estimation of glucose from urine sample: Spiking the urine with glucose 18 mg mL^{-1} was done before taking it for evaluation since it is the only carbohydrate which can be easily detected in urine. Comparison of the signals specifically the peak area and peak height was implemented to allow for study of the recovery yield for glucose. A comparison of the HPLC chromatograms of glucose following its extraction with a retention period of 3 min with direct injection of spiked sample without extraction is shown in Fig. 8. The results of the analysis indicated that there was an increase in the optimum height and peak area of glucose was increased. The enrichment in glucose content was after preconcentration through the application of the fabricated sorbent. These findings points to boronic acid functionality capturing the *cis*-diol compounds whereas the boronate affinity depends on the covalent reactions. For that reason the non-specific interactions induced adsorption can be inhibited through the selection of the relevant conditions that allows for optimum specificity.

Reproducibility and stability: An investigation of the reproducibility of the boronate affinity monolith was conducted taking into concept the conditions of relative standard deviation (RSD) for the retention time of glucose. The relative standard deviation for run-to-run was 4.81 % (n = 3) whereas the one for batch-to-batch of the monolithic sorbent was 5.63 % (n = 3), as shown in Fig. 9. Following the storage of monolith in MeOH:distilled water with a ratio of 50:50 for a period lasting three months, it is capable of retaining its original performance. The present study has also indicated AABPA-*co*-EDMA

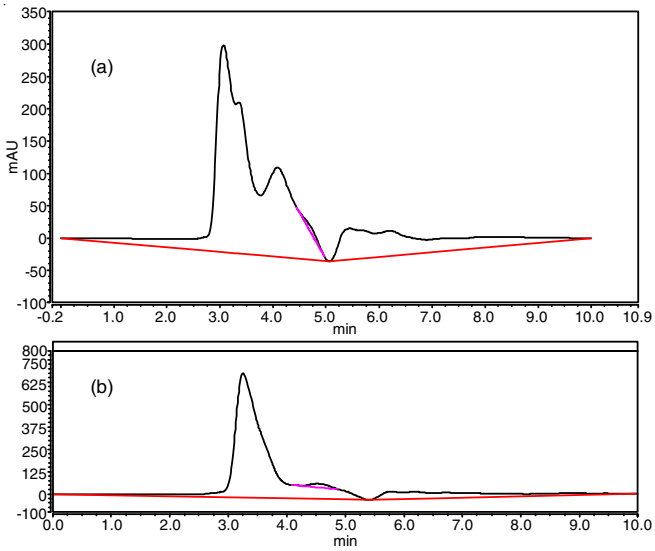

Fig. 8. Analysis of direct inject of glucose (18 mg mL^{-1}) spiked urine sample (a) and after preconcentration/purification using organic boronate affinity sorbent (b). The wavelength was set on 214 nm

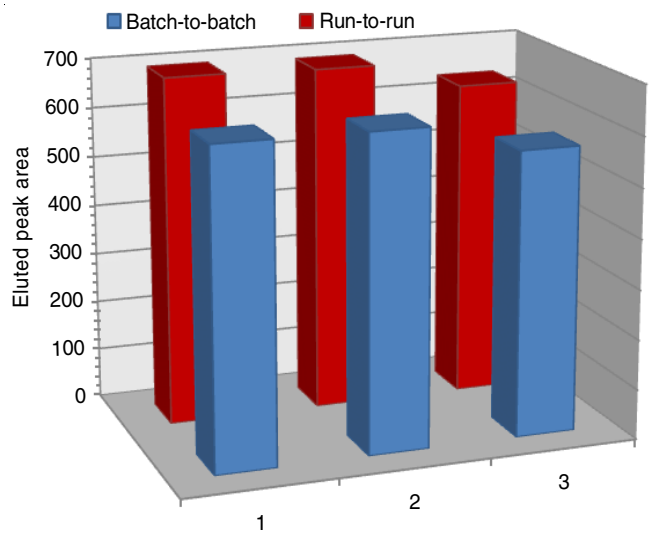

Fig. 9. Reproducibility of the fabricated boronate affinity sorbent

monolith to be stable thus facilitating the implementation of more than five analyses using similar composite monolith having a centimeter within the micropipette for over a week. Despite the complete procedure for extraction and desorption being relative long lasting 3 h and 25 min for routine analysis, the fabricated affinity boronate sorbent is applied in the pre-treatment of the various samples simultaneously. That is because the preparation reproducibility for fabricated affinity boronate sorbent is deemed suitable.

The drift in permeability is regarded to be the only observable drawback as it is integral in the loading of the solutions to the porous materials. That can in turn be attributed to the partial clogging of the inlet monolith following the long period of usage of the urine samples. Further, the boronic acids provides for a basic pH for substantial binding with *cis*-diols and as a result, fail in strongly binding with *cis*-diol containing compounds in near neutral or weak acidic samples such as serum. On the contrary, there are several benefits for the preparation of the boronate organic monolith with such being

simple procedure during fabrication, highly sensitive, strong reproducibility, highly permeable and environmentally friendly**.** As a result of these benefits, the AAPB organic monolithic materials possess huge potential in selection of promising applications.

Conclusion

In conclusion, the new boronate affinity monolithic sorbent that applies AAPBA as the boronate affinity ligand has been prepared successfully. Generally, the structure of the fabricated organic monolith has been characterized through promoting homogeneity and uniformity in pore distribution. The development of a polymeric boronate affinity monolith has been implemented selectively to aid in the preconcentration of the *cis*-diol compounds**.** The present study also identified that the AABPA-*co*-EDMA polymer monolith is porous, chemically stable and possess a long lifetime, whereas demonstrating excellent enrichment factors for pre-concentration of galactose and catechol. Additionally, the isolation of glucose from the urine sample was successfully implemented through the application of developed sorbent and the adoption of the capture and release procedure, which can be manipulated by selecting pH switch. Additionally, the high accuracy and precision was selected pointing to the success of the proposed method when adopted in the analysis of *cis*-diol containing compounds having good reliability. The on-line approach also presents an alternative practical tool in facilitating the sensitive determination of *cis*-diol containing compounds. Further, the suggested system is important for boronate affinity applications in real sample of genomics or for the valuable *cis*-diol at low concentrations which are recovered in low-volume samples.

CONFLICT OF INTEREST

The authors declare that there is no conflict of interests regarding the publication of this article.

REFERENCES

1. A. Ivanov, N.M. Solodukhina, L. Nilsson, M.P. Nikitin, P.I. Nikitin, V.P. Zubov and A.A. Vikhrov, *Polym. Sci. Ser. A*, **54**, 1 (2012); https://doi.org/10.1134/S0965545X12010026.
2. H. Zhu, H. Yao, K. Xia, J. Liu, X. Yin, W. Zhang and J. Pan, *Chem. Eng. J.*, **346**, 317 (2018); https://doi.org/10.1016/j.cej.2018.03.170.
3. J. Turková, Bioaffinity chromatography, Elsevier, vol. 55 (1993).
4. I. Abreu-Sánchez, New Targets in Plant Boron Deficiency Response: N-Glycosylation and Regulation of Root Development (2016).
5. S. Jin, W. Zhang, Q. Yang, L. Dai and P. Zhou, *Talanta*, **178**, 710 (2018); https://doi.org/10.1016/j.talanta.2017.10.011.
6. D. Li, Y. Chen and Z. Liu, *Chem. Soc. Rev.*, **44**, 8097 (2015); https://doi.org/10.1039/C5CS00013K.
7. Y. Zhang, H. Yin and H. Lu, *Glycoconj. J.*, **29**, 249 (2012); https://doi.org/10.1007/s10719-012-9398-x.
8. Y. Zhang, X. Xie, X. Zhao, F. Tian, J. Lv, W. Ying and X. Qian, *J. Proteomics*, **170**, 14 (2018); https://doi.org/10.1016/j.jprot.2017.09.014.
9. H. Xiao, F. Sun, S. Suttapitugsakul and R. Wu, *Mass Spectrom. Rev.*, (2019); https://doi.org/10.1002/mas.21586.
10. D. Medina-Cano, E. Ucuncu, L.S. Nguyen, M. Nicouleau, J. Lipecka, J.-C. Bizot, C. Thiel, F. Foulquier, N. Lefort, C. Faivre-Sarrailh, L. Colleaux, I.C. Guerrera and V. Cantagrel, *eLife*, **7**, e38309 (2018); https://doi.org/10.7554/eLife.38309.
11. D.E. McCoy, T. Feo, T.A. Harvey and R.O. Prum, *Nat. Commun.*, **9**, 1 (2018); https://doi.org/10.1038/s41467-017-02088-w.
12. H. Li and Z. Liu, *TrAC Trends Anal. Chem.*, **37**, 148 (2012); https://doi.org/10.1016/j.trac.2012.03.010.
13. D.F. Zielinska, F. Gnad, J.R. Wiœniewski and M. Mann, *Cell*, **141**, 897 (2010); https://doi.org/10.1016/j.cell.2010.04.012.
14. J.S. Fossey, F. D'Hooge, J.M.H. van den Elsen, M.P. Pereira Morais, S.I. Pascu, S.D. Bull, F. Marken, A.T.A. Jenkins, Y.-B. Jiang and T.D. James, *Chem. Rec.*, **12**, 464 (2012); https://doi.org/10.1002/tcr.201200006.
15. E. Alzahrani and K. Welham, *Analyst*, **136**, 4321 (2011); https://doi.org/10.1039/c1an15447h.
16. E. Alzahrani and K. Welham, *Anal. Chim. Acta*, **798**, 40 (2013); https://doi.org/10.1016/j.aca.2013.08.035.
17. E. Alzahrani and K. Welham, *Analyst*, **137**, 4751 (2012); https://doi.org/10.1039/c2an16018h.
18. R. Nishiyabu, Y. Kubo, T.D. James and J.S. Fossey, *Chem. Commun.*, **47**, 1106 (2011); https://doi.org/10.1039/c0cc02920c.
19. X.-C. Liu and W.H. Scouten, Boronate Affinity Chromatography, In: Affinity Chromatography, Springer, pp. 119-128 (2000).
20. X. Ling and Z. Chen, *Anal. Bioanal. Chem.*, **410**, 501 (2018); https://doi.org/10.1007/s00216-017-0740-9.
21. L. Ren, Z. Liu, M. Dong, M. Ye and H. Zou, *J. Chromatogr. A*, **1216**, 4768 (2009); https://doi.org/10.1016/j.chroma.2009.04.036.
22. G. Wulff, *Pure Appl. Chem.*, **54**, 2093 (1982); https://doi.org/10.1351/pac198254112093.
23. G. Wulff, M. Lauer and H. Böhnke, *Angew. Chem. Int. Ed. Engl.*, **23**, 741 (1984); https://doi.org/10.1002/anie.198407411.
24. S. Jin, L. Liu and P. Zhou, *Mikrochim. Acta*, **185**, 308 (2018); https://doi.org/10.1007/s00604-018-2824-4.
25. A. Matsumoto, K. Yamamoto, R. Yoshida, K. Kataoka, T. Aoyagi and Y. Miyahara, *Chem. Commun.*, **46**, 2203 (2010); https://doi.org/10.1039/b920319b.
26. M. Dowlut and D.G. Hall, *J. Am. Chem. Soc.*, **128**, 4226 (2006); https://doi.org/10.1021/ja057798c.
27. A. Pal, M. Bérubé and D.G. Hall, *Angew. Chem. Int. Ed.*, **49**, 1492 (2010); https://doi.org/10.1002/anie.200906620.
28. L. Ren, Y. Liu, M. Dong and Z. Liu, *J. Chromatogr. A*, **1216**, 8421 (2009); https://doi.org/10.1016/j.chroma.2009.10.014.
29. M. Chen, Y. Lu, Q. Ma, L. Guo and Y.-Q. Feng, *Analyst*, **134**, 2158 (2009); https://doi.org/10.1039/b909581k.
30. Y. Xu, Z. Wu, L. Zhang, H. Lu, P. Yang, P.A. Webley and D. Zhao, *Anal. Chem.*, **81**, 503 (2009); https://doi.org/10.1021/ac801912t.
31. J. Liu, K. Yang, Y. Qu, S. Li, Q. Wu, Z. Liang, L. Zhang and Y. Zhang, *Chem. Commun.*, **51**, 3896 (2015); https://doi.org/10.1039/C4CC10004B.
32. M. Khanal, T. Vausselin, A. Barras, O. Bande, K. Turcheniuk, M. Benazza, V. Zaitsev, C.M. Teodorescu, R. Boukherroub, A. Siriwardena, J. Dubuisson and S. Szunerits, *ACS Appl. Mater. Interfaces*, **5**, 12488 (2013); https://doi.org/10.1021/am403770q.
33. O.G. Potter, M.C. Breadmore and E.F. Hilder, *Analyst*, **131**, 1094 (2006); https://doi.org/10.1039/b609051f.
34. C. Wu, Y. Liang, Q. Zhao, Y. Qu, S. Zhang, Q. Wu, Z. Liang, L. Zhang and Y. Zhang, *Chem. Eur. J.*, **20**, 8737 (2014); https://doi.org/10.1002/chem.201402787.
35. D. Li, Y. Li, X. Li, Z. Bie, X. Pan, Q. Zhang and Z. Liu, *J. Chromatogr. A*, **1384**, 88 (2015); https://doi.org/10.1016/j.chroma.2015.01.050.
36. X.-J. Li, M. Jia, Y.-X. Zhao, Z.-S. Liu and H. Akber Aisa, *J. Chromatogr. A*, **1438**, 171 (2016); https://doi.org/10.1016/j.chroma.2016.02.031.
37. X. Hou, W. Huang, F. Zhu, F. Geng and M. Tian, *Anal. Methods*, **11**, 317 (2019); https://doi.org/10.1039/C8AY02311E.
38. W. Zhang, W. Liu, P. Li, X. Xiao, H. Wang and B. Tang, *Angew. Chem. Int. Ed.*, **53**, 12489 (2014); https://doi.org/10.1002/anie.201405634.
39. W. Huang, X. Hou, Y. Tong and M. Tian, *RSC Adv.*, **9**, 5394 (2019); https://doi.org/10.1039/C9RA00511K.
40. E. Alzahrani, *Int. J. Adv. Sci. Technical Res..*, **1**, 115 (2015).

41. Q. Li, C. Lü and Z. Liu, *J. Chromatogr. A*, **1305**, 123 (2013); https://doi.org/10.1016/j.chroma.2013.07.007.
42. D. Sýkora, P. Rezanka, K. Záruba and V. Král, *J. Sep. Sci.*, **42**, 89 (2019); https://doi.org/10.1002/jssc.201801048.
43. X. Wang, N. Xia and L. Liu, *Int. J. Mol. Sci.*, **14**, 20890 (2013); https://doi.org/10.3390/ijms141020890.
44. R. Wu, H. Zou, H. Fu, W. Jin and M. Ye, *Electrophoresis*, **23**, 1239 (2002); https://doi.org/10.1002/1522-2683(200205)23:9<1239::AID-ELPS1239>3.0.CO;2-X.
45. E. Alzahrani, *Int. J. Adv. Sci. Technical Res.*, **1,** 209 (2015).
46. E. Alzahrani, *Int. J. Adv. Eng. Nano Technol.*, **2**, 13 (2014).
47. E. Alzahrani, *Eng. Technol.*, **1**, 138 (2015).
48. K. Lacina, P. Skládal and T.D. James, *Chem. Cent. J.*, **8**, 60 (2014); https://doi.org/10.1186/s13065-014-0060-5.
49. M.B. Espina-Benitez, J. Randon, C. Demesmay and V. Dugas, *Sep. Purif. Rev.*, **47**, 214 (2018); https://doi.org/10.1080/15422119.2017.1365085.
50. H. Zheng, H. Lin, J. Sui, J. Yin, B. Wang, T.R. Pavase and L. Cao, *Chem. Select*, **4**, 623 (2019); https://doi.org/10.1002/slct.201801261.
51. I. Perçin, N. Idil and A. Denizli, *Colloids Surf. B Biointerfaces*, **162**, 146 (2018); https://doi.org/10.1016/j.colsurfb.2017.11.044.
52. Y. Liu, L. Ren and Z. Liu, *Chem. Commun.*, **47**, 5067 (2011); https://doi.org/10.1039/c0cc05675h.
53. Z. Liu and H. He, *Acc. Chem. Res.*, **50**, 2185 (2017); https://doi.org/10.1021/acs.accounts.7b00179.
54. A. Jönsson, R.R. Svejdal, N. Bøgelund, T.T.T.N. Nguyen, H. Flindt, J.P. Kutter, K.D. Rand and J.P. Lafleur, *Anal. Chem.*, **89**, 4573 (2017); https://doi.org/10.1021/acs.analchem.6b05103.
55. K. Sitthisinthu, Small Molecule Analysis on a Modified Hydrophillic Interaction Liquid Chromatography (HILIC) Monolith Using Micro-HPLC and Capillary Electrochromatography (CEC), King's College: London (2015).
56. H. Li, H. Wang, Y. Liu and Z. Liu, *Chem. Commun.*, **48**, 4115 (2012); https://doi.org/10.1039/c2cc30230f.
57. F. Svec and C.G. Huber, Monolithic Materials: Promises, Challenges, Achievements, ACS Publications (2006).
58. Á. Sáfrány, B. Beiler, K. László and F. Svec, *Polymer*, **46**, 2862 (2005); https://doi.org/10.1016/j.polymer.2005.02.024.
59. J.L. DoresSousa, A. Fernández-Pumarega, J. De Vos, M. Lämmerhofer, G. Desmet and S. Eeltink, *J. Sep. Sci.*, **42**, 522 (2019); https://doi.org/10.1002/jssc.201801092.
60. Z. Zajickova and I. Spánik, *J. Sep. Sci.*, **42**, 999 (2019); https://doi.org/10.1002/jssc.201801071.
61. M. Vázquez and B. Paull, *Anal. Chim. Acta*, **668**, 100 (2010); https://doi.org/10.1016/j.aca.2010.04.033.
62. K. Chuda, J. Jasik, J. Carlier, P. Tabourier, C. Druon and X. Coqueret, *Radiat. Phys. Chem.*, **75**, 26 (2006); https://doi.org/10.1016/j.radphyschem.2005.06.007.
63. W.-L. Fang, L.-J. Xia, X. Huang, X.-F. Guo, J. Ding, H. Wang and Y.-Q. Feng, *Chromatographia*, **81**, 1381 (2018); https://doi.org/10.1007/s10337-018-3592-3.
64. Y. Zhang, M. Mei, X. Huang and D. Yuan, *Anal. Chim. Acta*, **899**, 75 (2015); https://doi.org/10.1016/j.aca.2015.10.004.